Simulation of Lipofilling Reconstructive Surgery Using Coupled Eulerian Fluid and Deformable Solid Models

Vincent Majorczyk, Stéphane Cotin, Christian Duriez, and Jeremie Allard

Inria Nord-Lille Europe, France

Abstract. We present a method to simulate the outcome of reconstructive facial surgery based on fat-filling. Facial anatomy is complex: the fat is constrained between layers of tissues which behave as walls along the face; in addition, connective tissues that are present between these different layers also influence the fat-filling procedure. To simulate the end result, we propose a method which couples a 2.5D Eulerian fluid model for the fat and a finite element model for the soft tissues. The two models are coupled using the computation of the mechanical compliance matrix. Two contributions are presented in this paper: a solver for fluids which couples properties of solid tissues and fluid pressure, and an application of this solver to fat-filling surgery procedure simulation.

Keywords: Simulation, fluid-solid interaction, reconstructive surgery.

1 Introduction

The Parry-Romberg syndrome is a progressive hemifacial atrophy. It is due to disorders of central nervous system and is characterized by a degeneration of tissues beneath the skin. The syndrome affects generally one side of the face and distorts the nose and the mouth. Causes are still unknown, an autoimmune mechanism is suspected. The reconstructive surgery is the only way to restore the face with the adding of fat. In addition, there are less severe cases of facial dystrophy due to side effect of drugs or insulin-resistance for which drug solutions are not considered sufficient compared with reconstructive surgery [1].

The fat-filling procedure consists of injecting fat in subcutaneous areas. The main literature concerning about the fat-filling surgery are the result analyses of the operation. Surgeons test different methods of injection, or different products, and they compare measures before the operation, short-term and long-term to define the viability of their method [2]. As it is difficult to predict the results, most of the time surgeons rely on their experience to plan the operation and calculate the required volume of fat. So the surgeon must become familiar with the possible depths of injection (subdermal, intramuscular, supraperiosteal), and the amounts of fat to get the desired change [3].

The facial anatomy is complex: there are many layers of tissues (skin, Superficial Musculo-Aponeurotic System ...) with different properties [4]. Futhermore, ligaments, nerves and blood vessels connect the layers, change the stiffness of

K. Mori et al. (Eds.): MICCAI 2013, Part III, LNCS 8151, pp. 299–306, 2013.

tissues and create obstacles for injected fat. Each patient has a particular anatomy, and surgeons may need help planning difficult cases.

The long-term aim of this project is to use simulation and patient specific data to predict the behavior of injected fat under the skin. So the anatomy needs to be modelized realistically [5] to understand the role of each element.

The model presented in this paper is an 2.5D eulerian fluid. The fluid is injected between two layers of tissues, moves along a curved surface and has a thickness. The fluid solver uses the compliance properties of the solid to calculate the pressure of fluid. This pressure acts to surfaces and deforms solids.

2 Related Works

In simulation, while we can find a large amount of works about breast augmentation, it mainly concerns implants [6] and not the fat injection. The aim of these works consists to plan the surgery operation, finds the best implant and predicts the result. These works use the finite element method to simulate deformable tissues. The reconstruction of facial atrophy may use computed-assisted lipofilling [7], it only considers the volume difference of fat between the original model and the wished result.

The simulation of fluid-structure coupling is often particularly challenging. Each problem depends on the aim of the simulation, on the required precision and on the available data. The coupling method often needs to be adapted.

In gynaecology, Karry [8] describes a model with viscous fluid between soft tissues. It concerns a microbicide gel injected in the vagina to analyze the repartition of gel due to the pressure of membranes. This model is composed of a viscous fluid between two deformable solids. However, the proposed model is restricted to the simple case of an homogeneous solid.

Lagrangian particle-based methods allow to describe volume of solid and fluid as particles and generate repulsive forces among particles [9]. Solenhaler *et al.* [10] fixes the problem of incompressibility, but introduces a costly iterative scheme.

Eulerian models have inherent difficulties to resolve moving domain boundaries. Moreover, the method needs to avoid fluid loss and to correctly transfer forces between fluid and solid. Klingner [11] defines the topology of the domain at each step-time and handles accurately the behaviour of boundaries. Other methods handle moving boundaries within an Eulerian grid by modeling partly filled cells [12–14].

3 Fluid-Solid Model

The fat flows along a surface between two layers of tissues. In this model the fat is considered as a fluid and tissues are represented by deformable solids. The purpose of this section is to describe the fluid-solid coupling.

3.1 Fluid Model

The fluid model needs to be physically realistic and stable to simulate fluid between two deformable surfaces. The base of the method is described in [15]: it is an Eulerian fluid model which consists of a velocity field and a pressure field. The domain of the surface is in the form of a staggered grid representation [16]. Further, the surface is curved, the model uses a distortion matrix to adapt data (velocities and pressure) from facial topology to unitary cells [17]. We extend the model to add a fluid height field and take it into account in all equations to obtain a 2.5D formulation.

The method considers a succession of four operations: computation of external forces, the diffusion to simulate viscosity, the advection for turbulence and the projection to force fluid incompressibility. Regarding fluid-solid interactions, it is important to detail the projection mechanism.

The projection step allows the input fluxes in a cell to be equal to the output fluxes. So there is neither surplus nor loss of matter. At the beginning of the step the error between input flux and output flux is computed (eq.1). The error is named divergence D and is the sum of flux around the cell. The flux is the velocity u_{edge} multiplied by the area A_{edge} between adjacent cells.

$$D_{cell} = \sum_{edge} A_{edge} u_{edge}(t) \tag{1}$$

The pressure is a scalar field of values defined within each cell. It creates an additional flux proportional to the pressure differences between adjacent cells. For an incompressible fluid, the pressure can be computed as the solution enabling the divergence of the resulting velocity field to be zero, i.e. the divergence of the fluxes introduced by difference of pressure within a cell P_{cell} and in an adjacent cell P_{adj} should counterbalance the initial cell divergences:

$$D_{cell} = \sum_{edge} A_{edge} \left(P_{cell} - P_{adj}\right) \tag{2}$$

By gathering the equations of all cells, we obtain a matrix system of the form:

$$\mathbf{d} = \mathbf{J}\mathbf{p} \tag{3}$$

Where $\mathbf{d}$ is a vector with the divergence values D_{cell}, $\mathbf{p}$ is a vector which contains pressure values P, and $\mathbf{J}$ is the assembling matrix which includes area coefficients A_{edge}.

3.2 Deformable Solid

Good visual results can be obtained with discrete approaches (like spring-mass or particles) that are very fast to compute but not physics-based. On the other hand, numerical solutions, like the finite element method, allow to integrate accurately the constitutive law (strain/stress relation) of the deformable solid. The computation cost of such methods could be highly reduced when using

corotational strain measure [18] which is valid for deformations with large transformation (displacement and rotation).

This formulation gives the possibility to compute the compliance matrix (inverse of the matrix of the dynamic system) which have a pivotal role in the interaction calculation [19]. Equation (eq.4) describes the dynamic of a non-linear deformable object with external constraints applied :

$$\mathbf{M}\dot{\mathbf{v}} = \mathbf{f}_{ext} - \mathbb{F}(q, v) + \mathbf{H}^T\lambda \tag{4}$$

where $\mathbf{M}$ is mass matrix, q and v are the position and velocity vectors. $\mathbb{F}$ is a function which describes the internal visco-elastic forces. $\mathbf{f}_{ext}$ is the external forces such as the gravity. λ is a vector of applied constraints forces, multiplied by a constraint space to mechanical space correspondence matrix $\mathbf{H}^T$.

The constraints are given as a set of (in)equations :

$$\delta = \left[\mathbf{H}\underbrace{\left(\frac{\mathbf{M}}{h^2} + \frac{d\mathbb{F}}{hdv} + \frac{d\mathbb{F}}{dq}\right)}_{\mathbf{K^{-1}}}\mathbf{H}^T\right]\lambda \tag{5}$$

δ corresponds to the desired constraint displacements and $\mathbf{K^{-1}}$, the inverse of matrix $\mathbf{K}$ which is homogeneous to stiffness matrix, is called the compliance matrix. So, (eq. 5) corresponds to the displacement of the fluid-solid interface due to forces applied on the object.

3.3 Fluid-Solid Coupling

We combine the above models to create a coupled system. The interactions between the fluid and the solid are handled by combining the fluid pressure and mechanical constraints equations.

From the point a view of the fluid, any motion of the solid which introduces height variations δ_h changes the incompressibility pressure equation (eq.3) into:

$$\mathbf{Jp} + \mathbf{A}\delta_h = \mathbf{d} \tag{6}$$

$\mathbf{A}$ is the matrix containing area coefficients converting height displacements to volumes. The height variation is a modification of the thickness of the fluid per time-step due to the pressure of the fluid on the solid. This volume change corresponds to having a flow normal to the surface of the cell. This flow is added to the divergence to compute the pressure.

From the point of view of the deformable solid, the coupling is considered as a set of constraints pushing on the surface exposed to the pressure of the fluid:

$$\lambda = \mathbf{A}^T\mathbf{p} \tag{7}$$

Combining with (eq.5), we obtain:

$$\delta_h = \mathbf{H}\mathbf{K}^{-1}\mathbf{H}^T\lambda \tag{8}$$

H is a matrix which adapts forces applied on the fluid-solid interface to the solid. That is to say, the fluid interface and the solid may have different topologies. Next, we merge (eq.7) and (eq.8) with the pressure equation (eq.6) :

$$\mathbf{Jp} + \underbrace{\left(\mathbf{AHK}^{-1}\mathbf{H}^T\mathbf{A}^T\right)}_{\mathbf{C}}\mathbf{p} = \mathbf{d} \tag{9}$$

C is a compliance expressed in the volume/pressure space. As the fluid is a closed domain, the above equation can be difficult to solve. To avoid this problem, we use numerical regularization and reinforcement of the diagonal of the matrix by replacing **C** with a regularization matrix **R** whose diagonal is the sum of all contributions of volume displacement on the domain (N cells) by a pressure on the considered cell i:

$$\mathbf{R}_{i,i} = \sum_{j=1}^{N} \mathbf{C}_{i,j} \tag{10}$$

$$(\mathbf{J} + \mathbf{R})\mathbf{p} = \mathbf{d} \tag{11}$$

The model allows to calculate pressure using fluid data and solid data. By introducing the matrix **R**, we have the volume changes of the fluid-film domain when applying pressure on the deformable walls. The role of this matrix is to provide some improvements to the numerical level: it essentially stabilizes the system and helps the convergence of the system. Thus, when solving this equation, we guaranty the incompressibility of the fluid. Finally, the pressures are transformed to forces to affect the motion of the deformable tissues.

4 Results

4.1 Simple Square

We first tested the behavior of our model on a square domain, where the fluid is placed between a rigid solid and a deformable solid. The simulation starts with an tunnel-like fluid volume in the center. The displacement over time of the fluid-solid surface is given in Fig.1. It shows a convergence of results with the use of different time-steps and mesh resolutions. The third graph corresponds to simulations with different stiffness. The simulations shows the coherence of the mathematical model: wherther spatial, temporal, respect of fluid incompressibility or general behavior.

4.2 Facial Fat-Filling

To validate our simulation on actual patient data, we start with a geometrical mesh of part of the face around the jaw. This three-dimensional mesh is obtained by laser scan of the skin of the patient's face. The surface mesh is then extruded and three layers of different tissues (skin, subcutaneous and SMAS[1].) are created

[1] Superficial Muscular Aponeurotic System

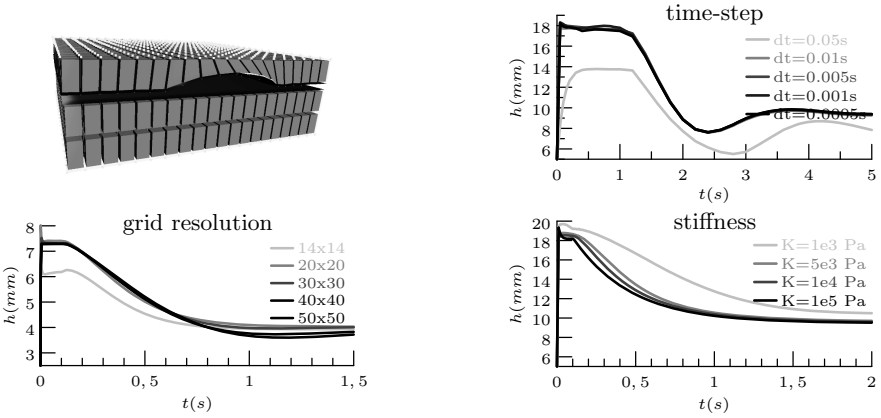

Fig. 1. Test simulation with a simple square (bottom layer: rigid ; top layer: deformable). The graphs show simulation results with different time-step, resolution and rigidity (Young's Modulus); curves represent the height of fluid over time of a point at the center of the square.

as hexahedral meshes. These meshes support a finite element computation of the tissue deformation, where the constitutive law is based on geometrically non linear elasticity (large displacements, small strains). Mechanical parameters (Young's modulus) of each layer is derived from data available in the literature: muscle 0.5 MPa [20], skin between 0.09 MPa [22] and 0.5 MPa [21]. The fat may be injected between any of the two layers. Adding fat near the skin modifies locally the shape of the cheek and adding fat near the SMAS corrects more globally the shape. Each layer is attached to one another by constraints to create zones separated by ligaments or walls.

The simulation illustrated in Fig.2 is composed of two layers of tissues (muscle and skin) and we inject fat to fill two zones: at the masseter and at the angle of inferior maxillary, corresponding to a good part of what was performed during the actual surgery. The simulated fat injection deforms the tissues based on the fluid pressure and tissue stiffness, it generates a change in the shape of the cheek. Then we compared the result of the simulation to the actual shape of the patient after surgery. Fig.2 shows the resulting deformation and the comparison. Although some differences exist between our results of the simulated fat-filling and the surgical outcome, the deformations are similar and the behaviour of model provides realistic results.

4.3 Performance Measurements

The time-step used in the above simulations is 10 ms. The computation time for each step is 0.6 seconds on average. Obtaining the compliance matrix C is currently the most expensive operation, because it involves the inverse of the matrix K whose size is proportional to the number of nodes of the deformable model (1244 hehahedrons compose each layer and 220 cells for the fluid).

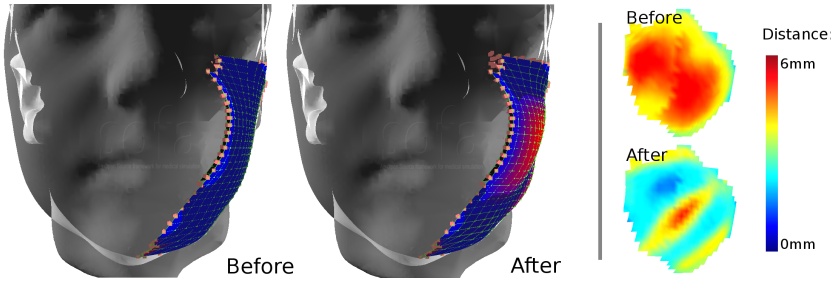

Fig. 2. Simulation with patient-specific data. The patient is suffering from Parry-Romberg syndrome. The blue zone is the simulated side. At the left, the patient before operation and the patient with simulated injection. At the right, is the Hausdorff distance with the result of surgical operation.

5 Conclusion

We presented a simulation method for fat-filling surgery procedure, based on a fluid-solid coupling interaction model. This model can take into account the variation in stiffness due to each patient anatomy.

Further works could be investigated in three areas : improving computational speed, handling large fluid viscosity, and using better ligament model and more generally a better knowledge of the anatomy. The computation speed could be significantly improved by optimizing the inversion of the mechanical stiffness matrix, or using one of several possible approximation methods. Fat is a really material in-between fluid and solid, but visco-elastic properties are not included in the fluid model. Afterwards, the model of tissue is constituted of layers which are constrained at many points to simulate obstacles. The constraints do not use properties of ligaments and should be more elastic. In addition, the tissue layers currently have a uniform thickness. The use of more accurate description of tissues should provide more realistic tissue behaviors.

Acknowledgements. The authors would like to thank Guillaume Captier, plastic surgeon at CHRU Montpellier, for providing us with the data. We would also like to thank Gerard Subsol and Benjamin Gilles, researchers at Montpellier Laboratory of Informatics, Robotics, and Microelectronics for their valuable feedback on this project.

References

1. Calmy, A., Bernasconi, E., Meier, C.A., Hirschel, B., Toutous-Trellu, L.: 10 years of lipodystrophy–and so many uncertainties. Rev. Med. Suisse 4(184), 2755–2757 (2008)
2. Fontdevila, J.J., et al.: Assessing the long-term viability of facial fat grafts: an objective measure using computed tomography. Aesthetic Surgery Journal 28(4), 380–386 (2008)

3. Coleman, S.R.: Structural Fat Grafting. Grabb and Smith's Plastic Surgery, 6th edn., pp. 480–485
4. Keeve, E., Girod, S., Kikinie, R., Girod, B.: Deformable Modeling of facial tissue for craniofacial surgery simulation. Comput. Aided Surg. 3(5), 228–238 (1998)
5. Mazza, E., Barbarino, G.G.: 3D mechanical modeling of facial soft tissue for surgery simulation. Facial Plast. Burg. Clin. North Am. 19(4), 523–537 (2011)
6. Lapuebla-Ferri, A.S., et al.: A patient-specific FE-based methodology to simulate prosthesis insertion during an augmentation mammoplasty. Medical Engineering and Physics 21, 1–9 (2011)
7. Hoehnke, C., Eder, M., Papadopulos, N.A., Zimmermann, A.: Minimal invasive reconstruction of posttraumatic hemi facial atrophy by 3-D computer-assisted lipofilling. Journal of Plastic, Reconstructive and Aesthetic Surgery 60, 1138–1144 (2007)
8. Karri, S.: 2D Thin-Film Flow of a Non-Newtonian Fluid Between Elastic Boundaries. Master-Thesis of the University of Kansas (2011)
9. Muller, M.: Fast and robust tracking of fluid surfaces. In: Proceedings of the 2009 ACM SIGGRAPH/Eurographics Symposium on Computer Animation, SCA 2009, pp. 237–245. ACM, New York (2009)
10. Solenthaler, B., Pajarola: Predictive-Corrective Incompressible SPH. ACM Transactions on Graphics 28(3), 401–406 (2009)
11. Klingner, B.: Fluid animation with dynamic meshes. In: SIGGRAPH 2006, pp. 820–825 (2006)
12. Johansen, H.: A cartesian grid embedded boundary method for poisson's equation on irregular domains. Journal of Computational Physics 147(1), 60–85 (1998)
13. Batty, C., Bertails, F., Bridson, R.: A fast variational framework for accurate solid-fluid coupling. ACM Trans. Graph. 26(3), 100 (2007)
14. Peskin, C.: The immersed boundary method. Acta Numerica 11, 479–517 (2002)
15. Stam, J.: Stable-fluids. In: SIGGRAPH 1999, pp. 121–128 (1999)
16. Fedkiw, R., et al.: Visual simulation of smoke. In: SIGGRAPH 2001, pp. 15–22 (2001)
17. Stam, J.: Flows on surfaces of arbitrary topology. ACM Transactions on Graphics 22(3), 724–731 (2003)
18. Muller, M., Gross, M.: Interactive virtual materials. In: Graphics Interface 2004, pp. 239–246 (2004)
19. Courtecuisse, H., Allard, J., Duriez, C., Cotin, S.: Preconditioner-based contact response and application to cataract surgery. In: Fichtinger, G., Martel, A., Peters, T. (eds.) MICCAI 2011, Part I. LNCS, vol. 6891, pp. 315–322. Springer, Heidelberg (2011)
20. Duck, F.: Physical properties of tissues: a comprehensive reference book. Academic Press, London (1991)
21. Samani, A., et al.: A 3D contact problem finite element model for breast shape deformation derived from mri data. In: ASB 1999 Annual Conference (1999)
22. Schnabel, J.A., et al.: Validation of non-rigid registration using finite element methods. In: Insana, M.F., Leahy, R.M. (eds.) IPMI 2001. LNCS, vol. 2082, pp. 344–357. Springer, Heidelberg (2001)